



# Application of a membrane condenser system for ammonia recovery from humid waste gaseous streams at a minimum energy consumption

Francesca Macedonio<sup>1</sup> · Mirko Frappa<sup>1</sup> · Omar Bamaga<sup>2</sup> · H. Abulkhair<sup>2,3</sup> · Eydah Almatrafi<sup>2,4</sup> · Mohammad Albeirutty<sup>2,3</sup> · Elena Tocci<sup>1</sup> · Enrico Drioli<sup>1</sup>

Received: 9 August 2021 / Accepted: 7 March 2022 / Published online: 4 April 2022  
© The Author(s) 2022

## Abstract

Among the various technologies for the removal and recovery of chemicals from gaseous streams, the membrane condenser (MCo) is proposed and analyzed in this work. In particular, the case of MCo used for the recovery of ammonia at minimum energy consumption is reported. For reaching this aim, three different MCo configurations have been proposed and compared. They differ in the way cooling is achieved: in configuration 1, the feed is cooled via cooling water before entering the membrane module; in configuration 2, a cold sweeping gas cools the feed stream directly inside the membrane module; in configuration 3, the feed is first partially cooled via an external medium and then a sweeping gas is used for the final cooling of the stream. The achieved results indicate configuration 2, among the three different proposed schemes, the one allowing to minimize energy consumption while permitting good water and chemicals recovery.

**Keywords** Membrane condenser · Ammonia recovery · Water recovery from waste gas

## Introduction

Ammonia is a harmful pollutant that is commonly produced in livestock facilities due to the breakdown of animal waste. Undigested feed protein and wasted feed are additional sources of ammonia in livestock systems. Many other sources may emit  $\text{NH}_3$  with a wide range of concentration, such as integrated coal gasification combined cycle power generation systems, landfills for waste disposal, crematory, chemical and manufacturing industries (Kim et al. 2007), and wastewater treatment plants (Hasegawa and Sato 1998; Wiwut et al. 2004; Xia et al. 2008). Ammonia is a color-less,

toxic, reactive and corrosive gas with a very sharp odor. The odor threshold for ammonia is between 5 and 20 ppm, and ammonia is regulated based on both unpleasant odor and health-related concerns (Sakuma et al. 2008). Emission of  $\text{NH}_3$  without appropriate treatment is causing frequent complaints from neighboring communities. Breathing levels of 50–100 ppm ammonia in the air can give rise to eye, throat and nose irritation. Moreover, nitrogen losses from composting material normally imply poor agronomical quality of the final compost and causes environmental pollution problems, such as acid rain (Buijsman et al. 1987; La Pagans et al. 2005). Ammonia emissions in a composting process of organic fraction of municipal solid wastes vary between 18 and 150  $\text{gNH}_3 \text{ Mg}^{-1}$  waste (Clemens and Cuhls 2003), while ammonia concentrations up to 700  $\text{mgNH}_3 \text{ m}^{-3}$  have been reported in exhaust gases from sludge composting (Haug 1993). To control malodor and protect the health of people working on animal farms and in the industries that use ammonia in their processes, waste gases containing ammonia are required to be treated in an efficient and viable process.

Another aspect to be considered is that ammonia dissolves easily in water. In water, most of the ammonia changes to ammonium, which is not a gas and does not smell. Ammonia

✉ Francesca Macedonio  
f.macedonio@itm.cnr.it

<sup>1</sup> Institute On Membrane Technology (CNR-ITM), via P. Bucci 17/C, 87036 Rende, CS, Italy

<sup>2</sup> Center of Excellence in Desalination Technology, King Abdulaziz University, Jeddah 21589, Saudi Arabia

<sup>3</sup> Mechanical Engineering Department, King Abdulaziz University, Jeddah 21589, Saudi Arabia

<sup>4</sup> Department of Mechanical Engineering, King Abdulaziz University, Jeddah 21589, Saudi Arabia

and ammonium can change back and forth in the water. In wells, rivers, lakes and wet soils, the ammonium form is the most common. People can taste ammonia in water at levels of about 35 ppm. Lower levels than this occur naturally in food and water.

Traditional strategies for reducing ammonia emissions from animal facilities and other sources include preventing ammonia formation and volatilization and controlling the transmission of ammonia. These strategies include the use of filtration systems (and/or biofiltration), impermeable and semi-permeable barriers, and dietary manipulation. Other conventional methods for  $\text{NH}_3$  removal from gas streams include absorption (wet scrubbing), adsorption and incineration (either thermal or catalytic) (Chang and Tseng 1996). Nevertheless, all these methods may have technical and/or economic limitations. In the last three decades, the applications of biological techniques increased because these techniques can overcome the operational limitations associated with the physicochemical treatment processes of waste air streams. Their main advantages are high ammonia removal, simplicity and low operation and maintenance costs (compared to physicochemical processes). Various studies confirm the ability of biofilters in the removal of ammonia from waste gas (Hort et al. 2009; Jun and Wenfeng 2009; Kim et al. 2000, 2007; La Pagans et al. 2005; Malhautier et al. 2003; Yasuda et al. 2009) from below 1 to around  $61 \text{ g NH}_3 \text{ m}^{-3} \text{ h}^{-1}$  (Moussavi et al. 2011). Despite the above-described advantages, the use of biofilters is constrained by some critical barriers. The most important drawbacks of biofiltration technology are the accumulation of contaminant degradation metabolites in the bed and thereby inhibiting the metabolic activity of the microorganisms. Furthermore, high pressure drops through the bed due to the growth and accumulation of biomass and degradation of media, and the large land area required to compensate for slow biodegradation, make this process expensive and uncompetitive. In addition, tracking the fate of ammonia removed is very complex and difficult.

On the other hand, ammonia has various uses so that global industrial production in 2018 was 175 million tonnes (Mineral Commodity Summaries 2020). Among the main uses of ammonia, the following are particularly worthy of note:

- *as fertilizer*: In the US as of 2019, approximately 88% of ammonia was used as fertilizers either as its salts, solutions or anhydrously. When applied to soil, it helps provide increased yields of crops such as maize and wheat. 30% of agricultural nitrogen applied in the US is in the form of anhydrous ammonia and *worldwide 110 million tonnes are applied each year*;
- *as precursor to nitrogenous compounds*;
- *as cleaner*;

- *in the fermentation*;
- *as antimicrobial agent for food products*.

Further, minor and emerging uses of ammonia are in the refrigeration, as a fuel, in textile (for treatment of cotton materials), as lifting gas, in the woodworking.

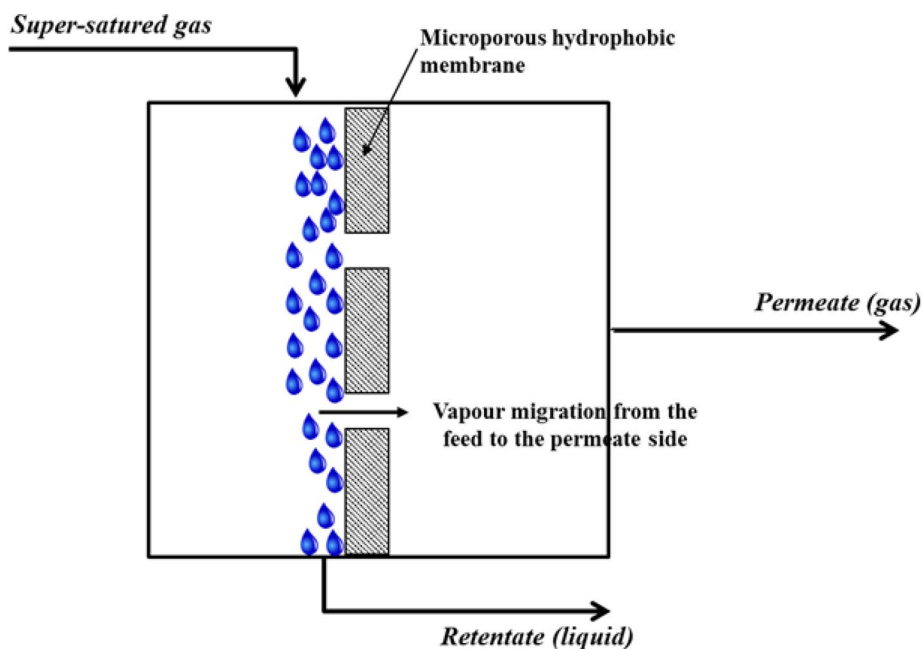
Objective of the present work is to consider membrane condenser (MCo) technology in order to remove ammonia from waste gaseous streams and, at the same time, to recover it in the liquid retentate stream. A modelling and simulation technique followed by experimental validation tests was adopted to predict the process performance of the membrane condenser (MCo) system in terms of water and ammonia recovery and specific energy consumption for three different MCo system configurations. The latter were analyzed with the aim to determine the one more energetically efficient to perform the desired ammonia recovery.

The working principle of MCo consists in condensing and recovering the water and the other condensable compounds contained in a gaseous stream on the retentate side of a membrane module, by exploiting the hydrophobic nature of the membrane (Macedonio et al. 2013, 2017, 2020). Due to the properties of the membrane, humidity and condensables of the feed are condensed and collected at the retentate side of the membrane, while the partially dehydrated gaseous stream passes to the permeate side (Fig. 1). Upstream to the membrane condenser contact surface, a transformation of the feed gas stream (e.g., by cooling) should be applied in order to reach a supersaturated state thus improving the amount of water that can be collected. On the retentate side, the compounds soluble in water will be retained in the collected liquid water as well (Macedonio et al. 2020). On the contrary, the permeate is a stream containing the gaseous compounds and the water molecules that have remained in the vapor phase and have passed through the pores of the membrane. Therefore, the MCo technology is not only limited to water recovery from humid waste gaseous streams, but also other main benefits can be achieved which include mitigation of the negative environmental impacts of waste gaseous streams containing hazardous air pollutants above permissible levels (such as ammonia) and, at the same time, their recovery in the liquid phase for their potential reuse.

The main advantages in using MCo compared to more widespread and traditional technologies are the following:

- The high simplicity and flexibility of the process whose operative conditions might be easily changed and adapted to the characteristics of the fed waste gaseous stream and/or to the amount of chemicals be recovered. For example, it will be shown that the amount of ammonia to be recovered can be increased by reducing the temperature of the membrane module feed. Moreover, in a MCo unit, the modulation of contact time between saturated stream

**Fig. 1** Membrane condenser principle (Macedonio et al. 2017)



and membrane, as well as the control of temperature and/or pressure difference between membrane sides, allow controlling the fraction of components present in the feed gaseous stream that will be retained in the condensed water.

- Small footprint because a MCo process is compact and estate saving. The available area between the retentate and permeate streams of a hollow fiber membrane module (as the one used in this work) is very large: the specific area with a fiber of  $10^{-3}$  mm inner diameter is about  $10^4$  m<sup>2</sup>/m<sup>3</sup> (Curcio et al. 2001), which offers the possibility of creating a compact device with a high geometrical surface enclosed in a small volume.
- High chemical resistance because the membranes can be fabricated from almost any chemically resistant polymers with hydrophobic intrinsic properties (such as polypropylene, polytetrafluoroethylene and polyvinylidene fluoride). As in all other membrane contactor processes, the membrane in MCo operation does not act as a sieve and does not react electrochemically with the feed stream.
- The MCo process offers the simultaneous recovery of water and condensable chemicals.
- Furthermore, remote control and easy automatic operations are other important characteristics of MCo process.

## Membrane condenser description

The description of membrane condenser as a new unit operation for the recovery of evaporated waste water can be found in (Macedonio et al. 2013, 2014). Briefly, the feed stream

(e.g., the waste gaseous stream) at a certain temperature is fed to the membrane module kept at a lower temperature for cooling the gas up to a supersaturation state. The water condenses in the membrane module and on the membrane surface where hydrophobic membranes are utilized to perform the separation (Fig. 1). The hydrophobic nature of the membranes not only avoids water droplets dragging, but also promotes vapor condensation exploiting the principle of dropwise condensation where, when condensation takes place on a surface that is not wet by the condensate, water beads up into droplets and rolls off the surface. Water vapor preferentially condenses on solid surfaces rather than directly from the vapor because of the reduced activation energy of heterogeneous nucleation in comparison with homogeneous nucleation (Enright et al. 2012; Kashchiev 2000).

In the two following sections, the model developed for simulating the MCo process and various possible MCo configurations are described.

## Membrane condenser model

In previous researches (Macedonio et al. 2013, 2014, 2020), simulation studies of the MCo process were carried out for predicting the membrane-based process performances (in terms of water recovery, energy consumption and liquid water concentration), and a plant in laboratory scale was built to verify the results achieved by the simulation analysis. Then, three different possible MCo configurations were compared in terms of amount of recovered liquid water and energy consumption (Macedonio et al. 2017).

In the present paper, the modeling and simulation of MCo process was developed in order to predict the process

performance also in terms of liquid water concentration in the three configurations announced in (Macedonio et al. 2017). The general objective was to identify a MCo design that would allow to have the best compromise not only in terms of process energy consumption and quantity of recovered water, but also as regards water concentration.

In particular, input values for the simulations are the morphological parameters of the membranes, the geometrical parameters of the modules and the properties (composition, flow rate, temperature and pressure) of the feed and cold medium (cold water and/or sweeping gas).

The values related to the feed are used for the calculation of the vapor pressure, relative humidity (RH) and dew point of the stream. Then, known the desired pressure for the flow gas at the entrance of the membrane condenser ( $P^{Condenser}$ ), the temperature, relative humidity and dew point of the waste gas at the exit of an eventual blower (required for compressing the feed gas before its entrance in the condenser) are calculated together with the power needed to drive the compression. The latter is estimated as follows:

$$Power = 2.78 \cdot 10^{-4} \frac{k}{k-1} F_v P^{Feed} \left[ \left( \frac{P^{Condenser}}{P^{Feed}} \right)^{\frac{k-1}{k}} - 1 \right]; [kw] \tag{1}$$

where  $k$  is the specific heat ratio ( $c_p/c_v$ ) of the feed,  $F_v$  is the volume flow rate of the feed gas at compressor inlet conditions,  $P^{Feed}$  is the feed pressure.

Afterward, the temperature ( $T^{Condenser}$ ) at the inlet of the condenser is calculated iteratively together with the physico-chemical properties of the waste gas and the supersaturation degree.

At the temperature  $T^{Condenser}$ , the flow rate of water vapor higher than the saturation limit condenses, and the amount of water that can be recovered from the feed is calculated accordingly to the following equation:

Water recovered fraction

$$= \frac{\left[ F_{H_2O}^{Feed} - \left( \frac{P_{H_2O}(F_{H_2O}^{Feed} - F_{H_2O}^{Feed})}{P - P_{H_2O}} - J_{H_2O}^{Permeating} \cdot A^{Membrane} \right) \right]}{F_{H_2O}^{Feed}} \tag{2}$$

where  $F_{H_2O}^{Feed}$  is the molar flow rate [ $mol s^{-1}$ ] of water in the feed,  $F^{Feed}$  is the total molar flow rate,  $P_{H_2O}$  is the partial pressure of water at the temperature  $T^{Condenser}$ , and  $A^{Membrane}$  is the membrane area.

The non-condensed water that still remains in the gas phase permeates through the membrane; it is considered by  $J_{H_2O}^{Permeating}$ , which is the water vapor flux through the membrane.

$J_{H_2O}^{Permeating}$  was calculated utilizing the reduced Knudsen molecular diffusion transition form of the Dusty-gas model:

$$J_{Total}^{Permeating} = -\frac{1}{RT} \left[ \frac{1}{D_{water}^{Knudsen}} + \frac{P_{air}}{PD_{water-air}} \right]^{-1} \frac{\Delta P_{Total}}{\delta}; [mol m^{-2} s^{-1}] \tag{3}$$

with Knudsen diffusivity calculated as:

$$D_{water}^{Knudsen} = \frac{2\epsilon r}{3\tau} \sqrt{\frac{8RT}{\pi M}}; [m^2 s^{-1}] \tag{4}$$

and the value of the quantity  $PD_{water-air}$  for water–air system is given by (Al-Odaidani et al. 2008; Bird et al. 1960; Lawson and Lloyd 1997):

$$PD_{water-air} = 4.46 * 10^{(-6)} \frac{\epsilon}{\tau} T^{2.334}; [Pa m^2 s^{-1}] \tag{5}$$

where

- $\Delta P$  is the water partial pressure difference through both membrane surfaces (i.e. it is the driving force to mass transfer in the proposed process), [Pa]
- $r$  is the membrane pore radius, [m]
- $\epsilon$  is the membrane porosity, [-]
- $\tau$  is the membrane tortuosity, [-]
- $\delta$  is the membrane thickness, [ $\mu m$ ]
- $R$  is the gas constant, [ $J kmol^{-1} K^{-1}$ ]
- $T$  is temperature of the module, [K]

The concentration of ammonia dissolved in the liquid water and recovered on retentate side  $c$  has been estimated through the following:

$$c = \frac{moli_{NH_3,FEED} - moli_{NH_3,OUT,perm}}{recovered\ water}$$

where  $moli_{NH_3,FEED}$  indicates the number of moles of  $NH_3$  in the feed (i.e. in the waste gaseous stream), and  $moli_{NH_3,OUT,perm}$  the number of moles of  $NH_3$  in the permeate.

The concentration  $c$  of ammonia in the retentate of the membrane condenser (i.e. in the flow of liquid leaving the process) is strictly influenced by the temperature in accordance with the following Henry’s law:

$$c = P_{NH_3}(T) \cdot H_{NH_3}(T)$$

where  $P_{NH_3}(T)$  and  $H_{NH_3}(T)$  are the partial pressure and the Henry’s law solubility constant of ammonia, respectively. The dependence of Henry’s constant on temperature is described with the following van’t Hoff equation:

$$H_{NH_3}(T) = H_{NH_3}^0 * \exp\left(\frac{-\Delta_{sol}H_{NH_3}}{R} \left(\frac{1}{T} - \frac{1}{T^0}\right)\right)$$

where  $\Delta_{\text{sol}}H_{\text{NH}_3}$  and  $H_{\text{NH}_3}^0$  are the enthalpy of dissolution and Henry’s law constant of ammonia at standard condition  $T^0$  (i.e. 298.15 K), respectively. Therefore, it is expected that  $c$  rises when the membrane module temperature ( $T$ ) decreases.

### Membrane condenser configurations

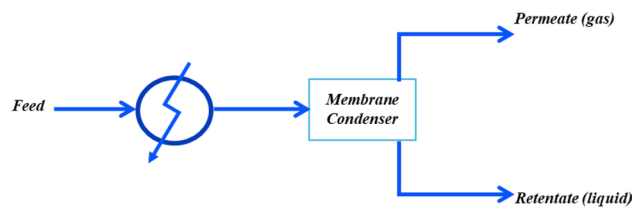
The fed gaseous stream has to be cooled either before entering or inside the membrane module. Three different MCo configurations have been studied, modeled and compared for individuating the one allowing to achieve the best compromise between energy consumption, amount and concentration of the recovered water. The three configurations differ in the way the feed is cooled (Fig. 2): in configuration 1, the feed is cooled via cooling water using a heat exchanger before entering the membrane module; in configuration 2, a cold sweeping gas cools the feed stream inside the membrane module through blowing the cold sweeping gas on the permeate side; in configuration 3, the feed is first partially cooled via an external medium, and then a sweeping gas is used for the final cooling of the stream. In configurations 2 and 3, the ratio between its flow rate and the feed flow rate is defined as the sweeping factor,  $I$ :

$$I = \frac{\text{cold sweeping gas flow rate}}{\text{feed waste gas flow rate}}$$

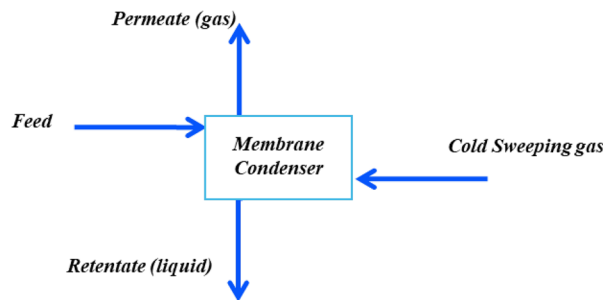
The algorithm considers either cooling water (when the fed gaseous stream has to be totally or partially cooled before entering the membrane module—configuration 1 and 3, respectively) or a cold sweeping gas (when the fed gaseous stream has to be totally or partially cooled inside the membrane module—configuration 2 and 3) as coolant medium.

In the case of cooling water, in this work, the algorithm considers a stream available at 32.2 °C and being returned at 40.0 °C, and it calculates the required cooling water flow rate, the area for heat exchange, the heat duty needed to cool the gaseous stream and to condense water vapor, the temperature of the gaseous stream at the exit of the heat exchanger together with the physicochemical properties of the gas and the supersaturation degree.

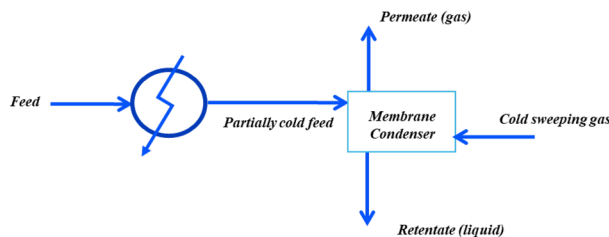
In the case of a cold sweeping gas, the algorithm supposes to utilize air at 20 °C and calculates the required parameters as stated above and also the power required to push the sweeping gas thus overcoming the pressure losses along the pipes and the membrane module. In both cases, counter-flow configurations (i.e. the fluids entering from opposite ends) were chosen since more efficient than parallel-flow configuration.



Configuration number 1.



Configuration number 2.



Configuration number 3.

Fig. 2 Schemes of the MCo configurations

### Experiments for model validation

A specifically designed and fabricated MCo experimental system was used for validating the model and verifying its capability to predict the quantity and concentration of water recovered under various operating conditions. The description of the MCo system can be found elsewhere (Macedonio et al. 2020). Briefly, the MCo system allows controlling the composition and flow rate of the humid gaseous stream fed to the membrane module, and it is equipped with all necessary sensors and instrumentation for data collection and storage. Microporous hydrophobic polypropylene commercial membranes are assembled in the module (made in stainless steel) by only one fixed end for an active membrane area of about 258 cm<sup>2</sup>. According to manufacturer’s data (Membrana), each membrane used (3 M™ Capillary Membrane MF-PP Series, Type S6/2) has inner diameter equal

to 1.8 mm, wall thickness of 450  $\mu\text{m}$  and nominal pore size of 0.20  $\mu\text{m}$ .

Table 1 summarizes the operating conditions used in the experiments.

The comparison between the results obtained through the simulations and those of the experimental measurements is shown in Fig. 3. The lines are referred to the simulations, the points to the experimental measurements. It can be appreciated the good agreement between theoretical and experimental results, both for water recovery and ammonia concentrations.

In the experiments as well as in the simulation,  $\Delta T$  indicates the temperature difference between the feed and the membrane module, and the increase in  $\Delta T$  shown in Figs. 3, 4, 5, 6, 8 and 9 is due to the reduction in the membrane module temperature (while the temperature of the feed is kept constant). It can be observed that as  $\Delta T$  grows, both the saturation and the solubility of ammonia in the liquid water increase and, as a consequence, water recovery and ammonia concentration increase, too (Fig. 3).

**Table 1** Operative conditions utilized in the experimental tests

Relative humidity, %	From 98.0 to 103.8
Feed temperature, $^{\circ}\text{C}$	From 34.9 to 35.3
Feed flow rate/membrane area = $Q/A$ , $\text{m h}^{-1}$	2.7
$\Delta T$ , $^{\circ}\text{C}$	From 2.5 to 11.6
$\text{NH}_3$ concentration in the feed, ppm	552

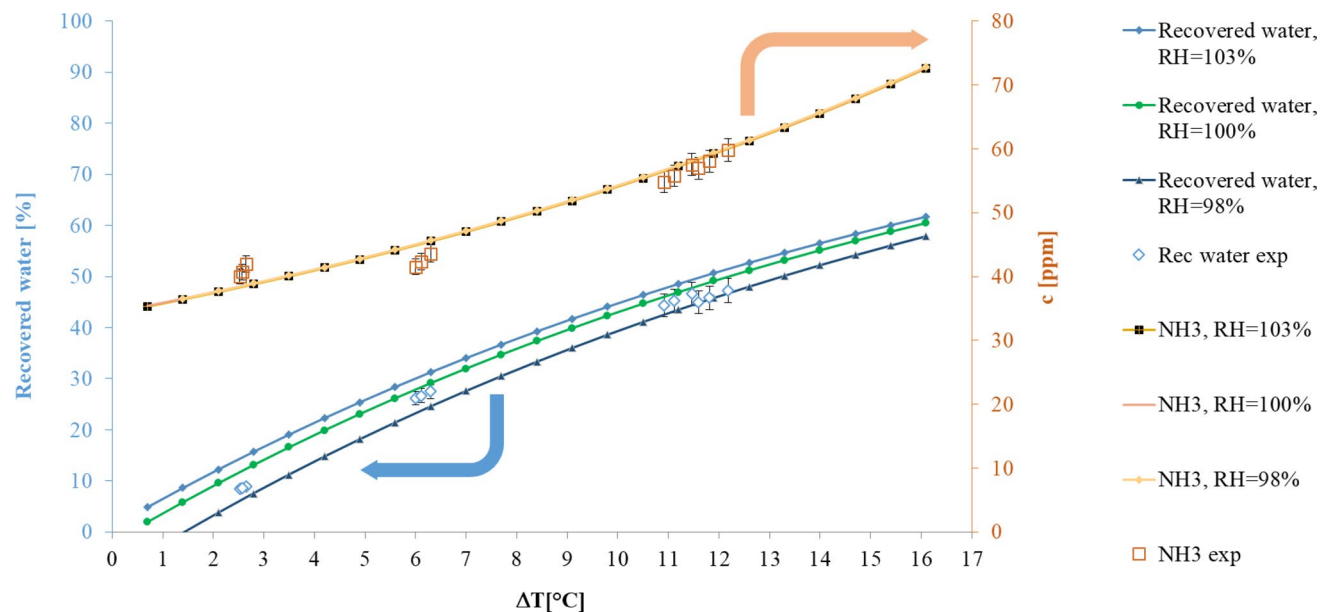


**Fig. 3** Recovered water and concentration versus  $\Delta T$ . Symbols: experimental results; lines: simulation results. (Experimental conditions:  $98.0\% \leq \text{RH}_{\text{Feed}} \leq 103.8\%$ ;  $34.9\text{ }^{\circ}\text{C} \leq T_{\text{Feed}} \leq 35.3\text{ }^{\circ}\text{C}$ ;

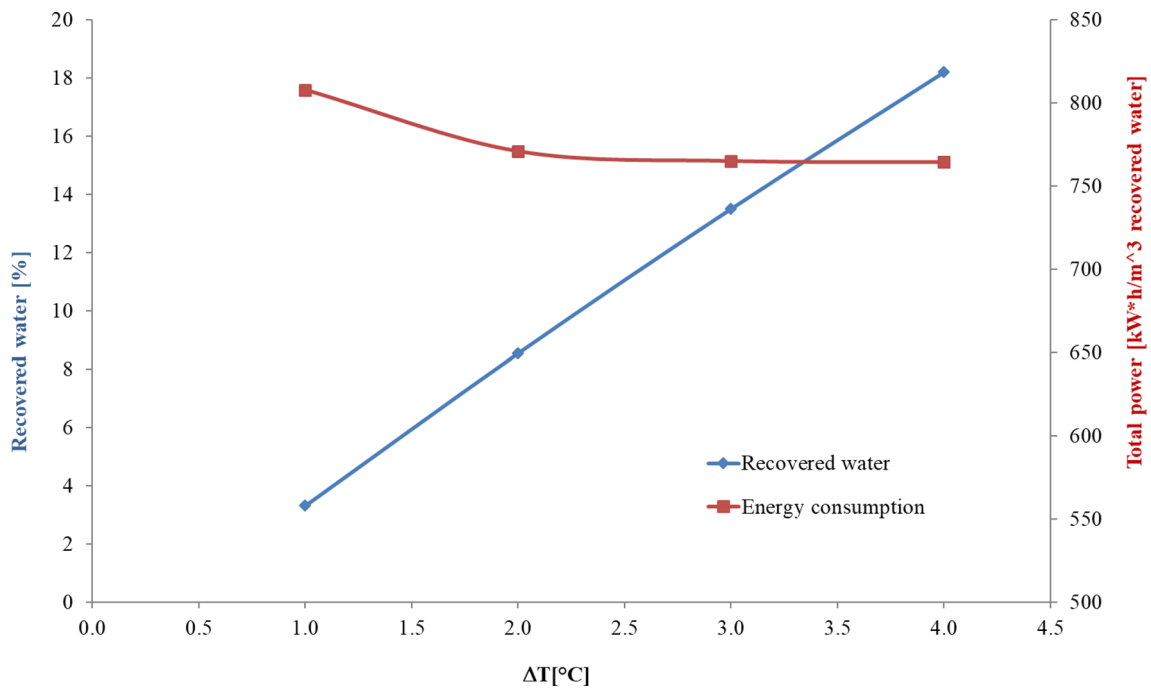
## Comparison among the various membrane condenser configurations

Figure 4 shows water recovery and energy consumption for configuration 1. It can be observed that while water recovery increases with growing  $\Delta T$ , energy consumption decreases initially at a higher rate, then it follows an almost constant value in the analyzed range of  $\Delta T$  (from 1 to 4  $^{\circ}\text{C}$ ). The detected trend has to be ascribed to the analyzed reduced  $\Delta T$  and to the fact that energy consumption is expressed with respect to the amount of recovered liquid water, which increases with  $\Delta T$ .

The disadvantage of configuration number 1 is linked to the medium utilized for cooling the feed, in particular when its temperature is low. The use of cooling water or surrounding air as a coolant medium is common in many conventional condensers. However, 5  $^{\circ}\text{C}$  is the approaching  $\Delta T$  in industrial plants. This implies that the amount of recovered water and the power needed to drive the process can be computed until when the temperature of the waste gas at the exit of the condenser is 5  $^{\circ}\text{C}$  higher than (or no more than equal to) the temperature of the discharged cooling water (which can be at most 40  $^{\circ}\text{C}$ ). Therefore, since the temperature of the feed is 45  $^{\circ}\text{C}$ , the maximum  $\Delta T$  is 4  $^{\circ}\text{C}$ . (This implies that the temperature of the waste gas at the exit of the condenser is 41  $^{\circ}\text{C}$ .)

Comparing the trend of recovered water and concentration with  $\Delta T$  in configuration 1 (Fig. 5), higher is the  $\Delta T$ ,

$2.5\text{ }^{\circ}\text{C} \leq \Delta T \leq 11.6\text{ }^{\circ}\text{C}$ ;  $\text{NH}_{3,\text{Feed}} = 522\text{ ppm}$ ;  $Q/A = 2.7\text{ m/h}$ . Model:  $98.0\% \leq \text{RH}_{\text{Feed}} \leq 103\%$ ;  $T_{\text{Feed}} = 35.1\text{ }^{\circ}\text{C}$ ;  $\text{NH}_{3,\text{Feed}} = 522\text{ ppm}$ ;  $Q/A = 2.7\text{ m/h}$ )



**Fig. 4** Recovered water and energy consumption versus  $\Delta T$  for configuration 1. Feed temperature = 45 °C; RH feed = 100%

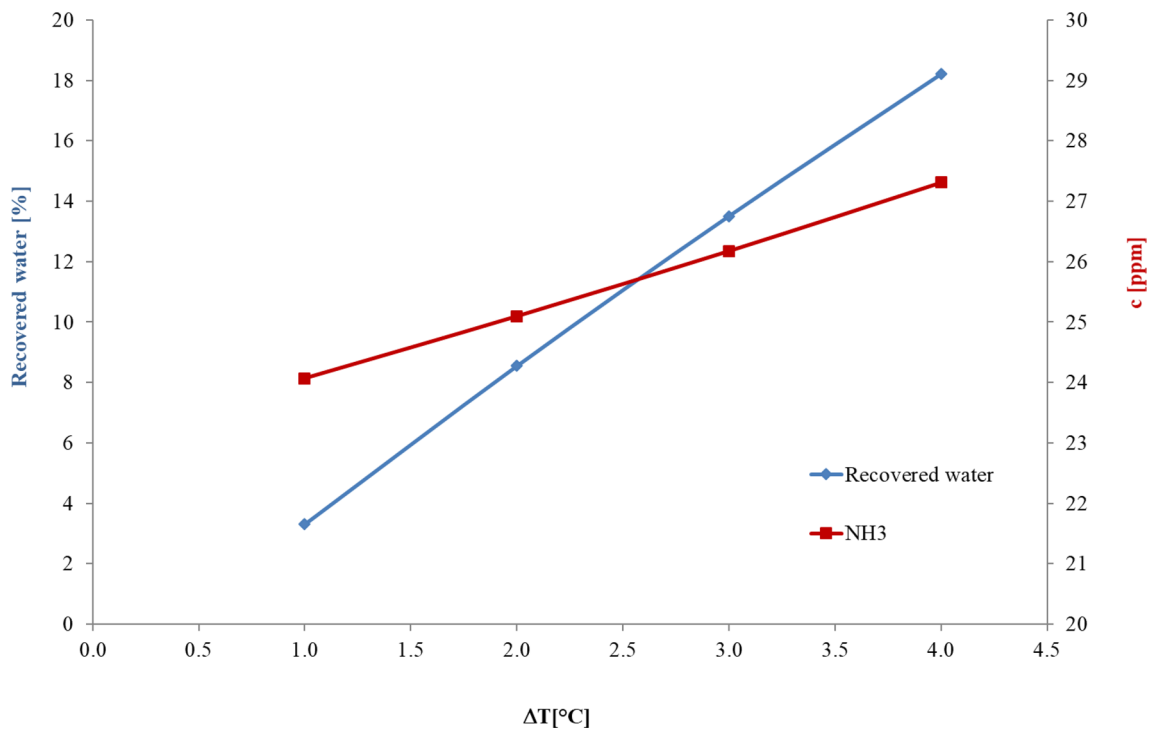
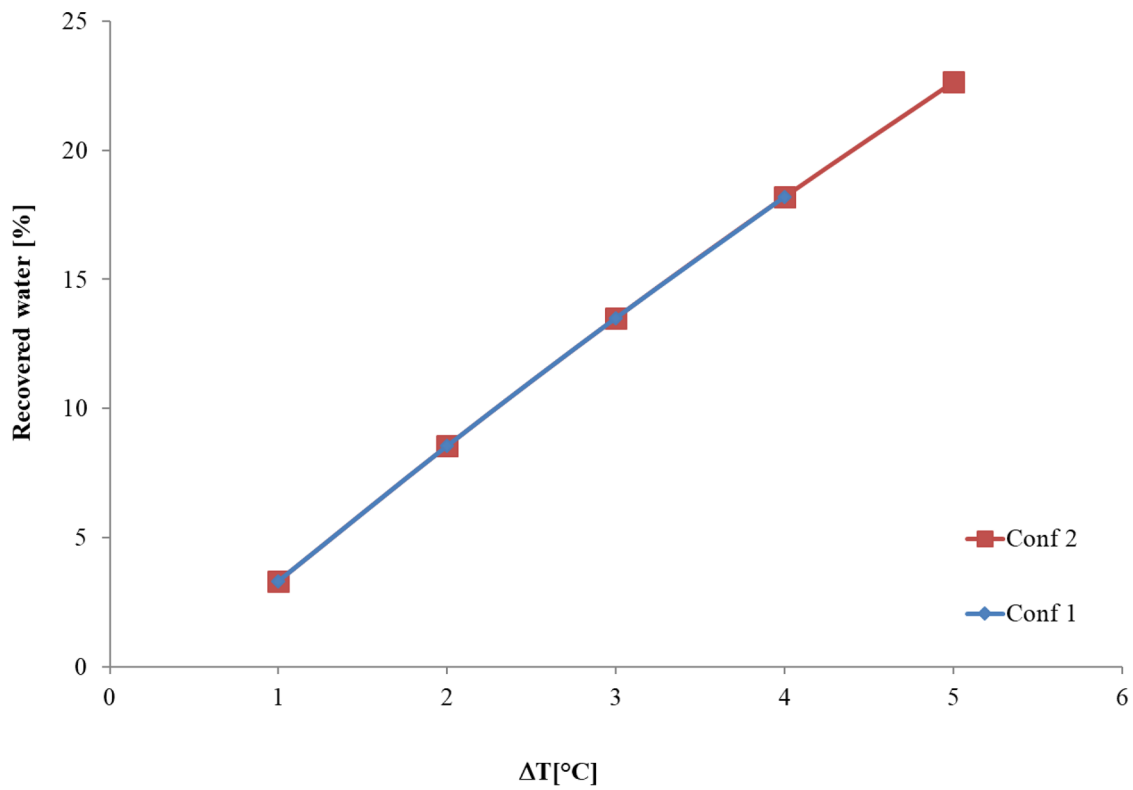


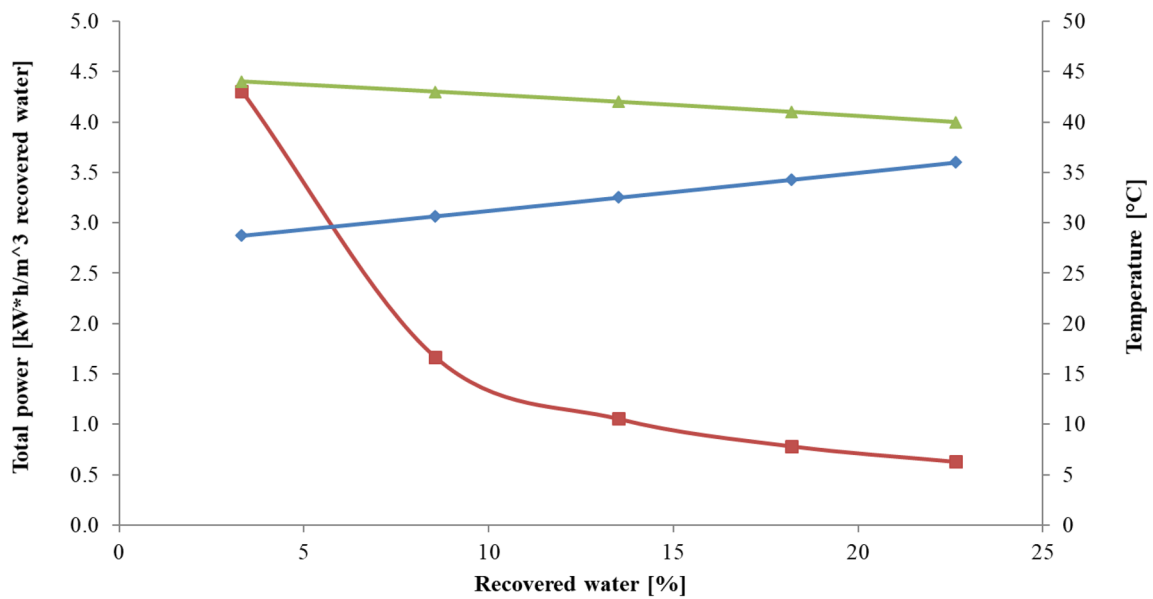
**Fig. 5** Recovered water and ammonia concentration (c) versus  $\Delta T$  for configuration 1. Feed temperature = 45 °C; RH feed = 100%

higher is the water recovery, as well as higher is NH<sub>3</sub> concentration in liquid water at minimum energy consumption (per m<sup>3</sup> of recovered water—Fig. 4).

As shown in Fig. 6, water recovery and energy consumption for configuration 2 (i.e. with a cold sweeping gas cooling the feed stream directly inside the membrane module) are reported. As in the previous case, the values reported



(a)



(b)

**Fig. 6** a Recovered water versus feed cooling gradient ( $\Delta T$ ) for configuration 1 and configuration 2 ( $I=3$ ) and b energy consumption for configuration 2 ( $I=3$ ). (Feed temperature = 45 °C; RH feed = 100%)



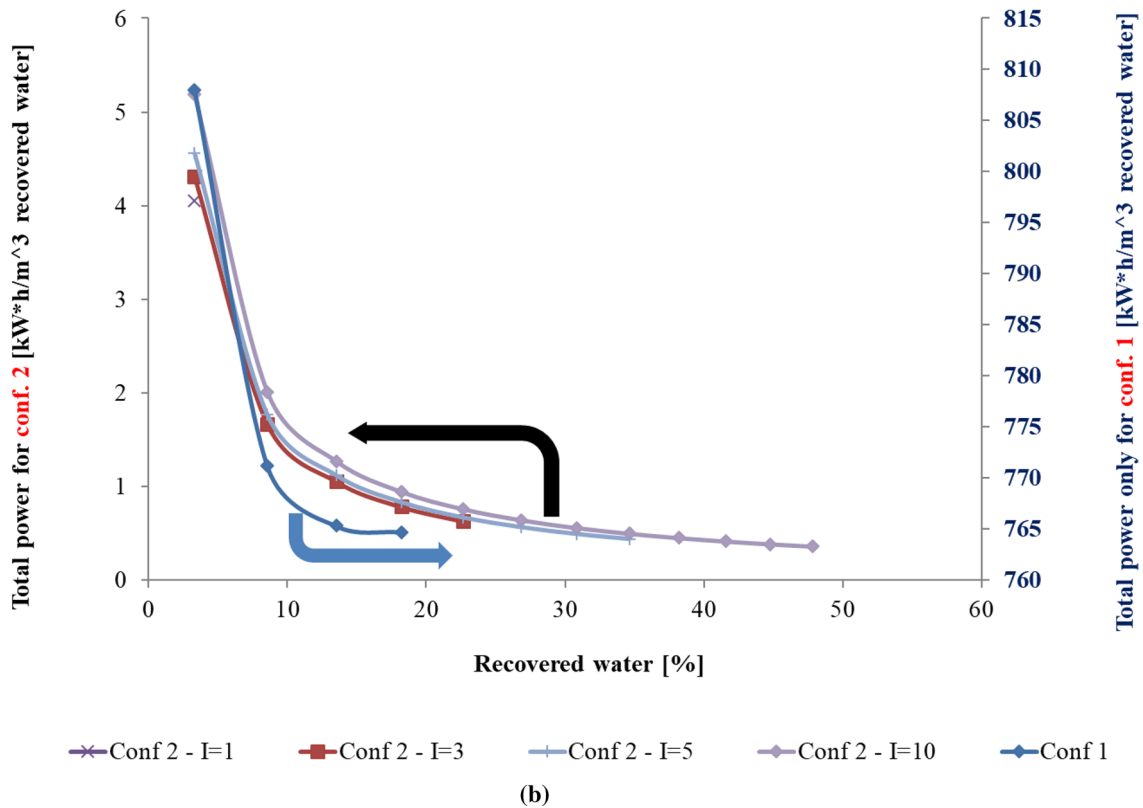
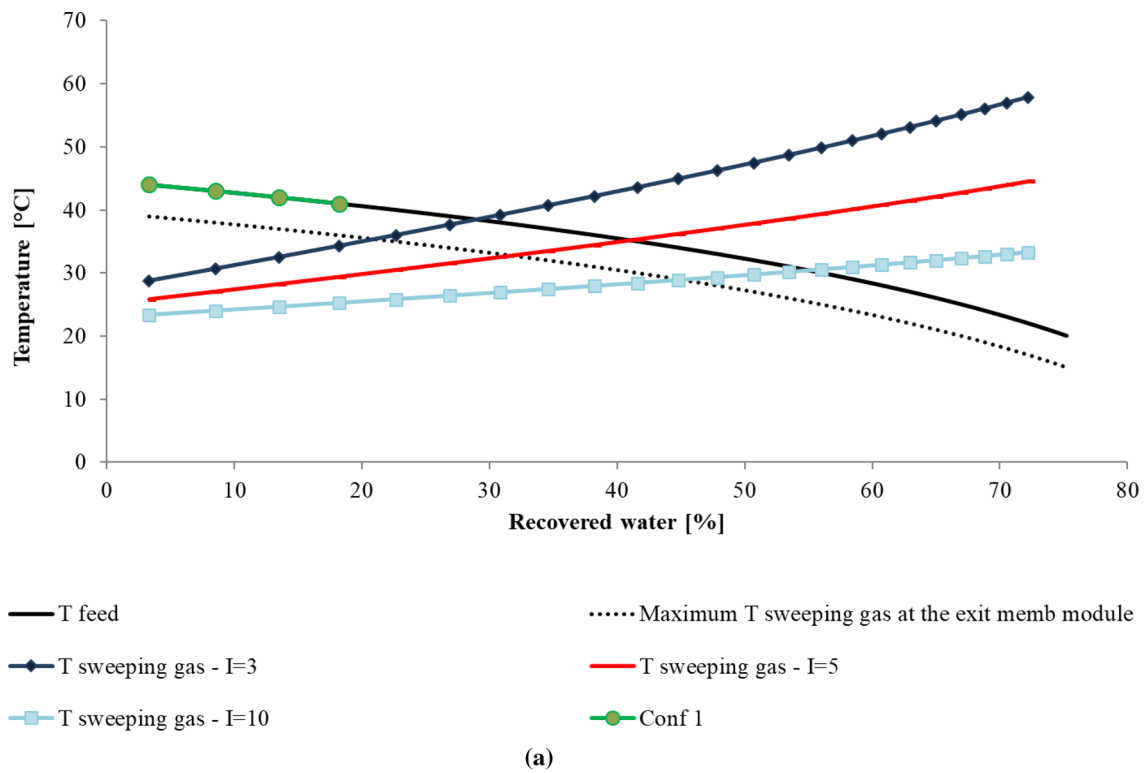
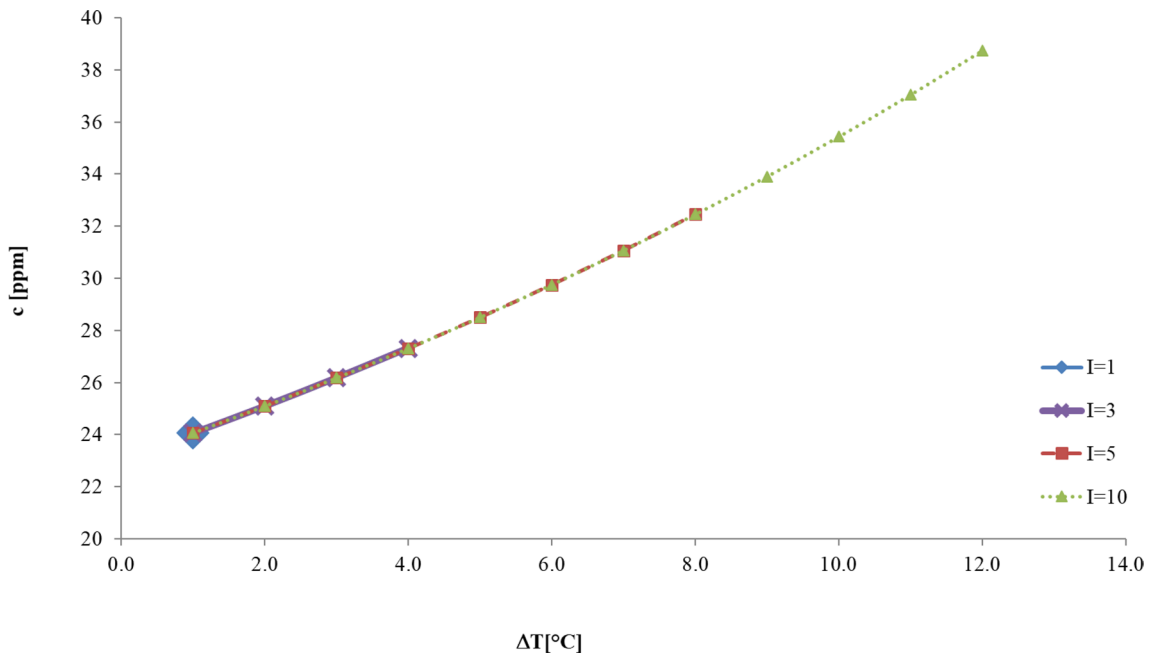
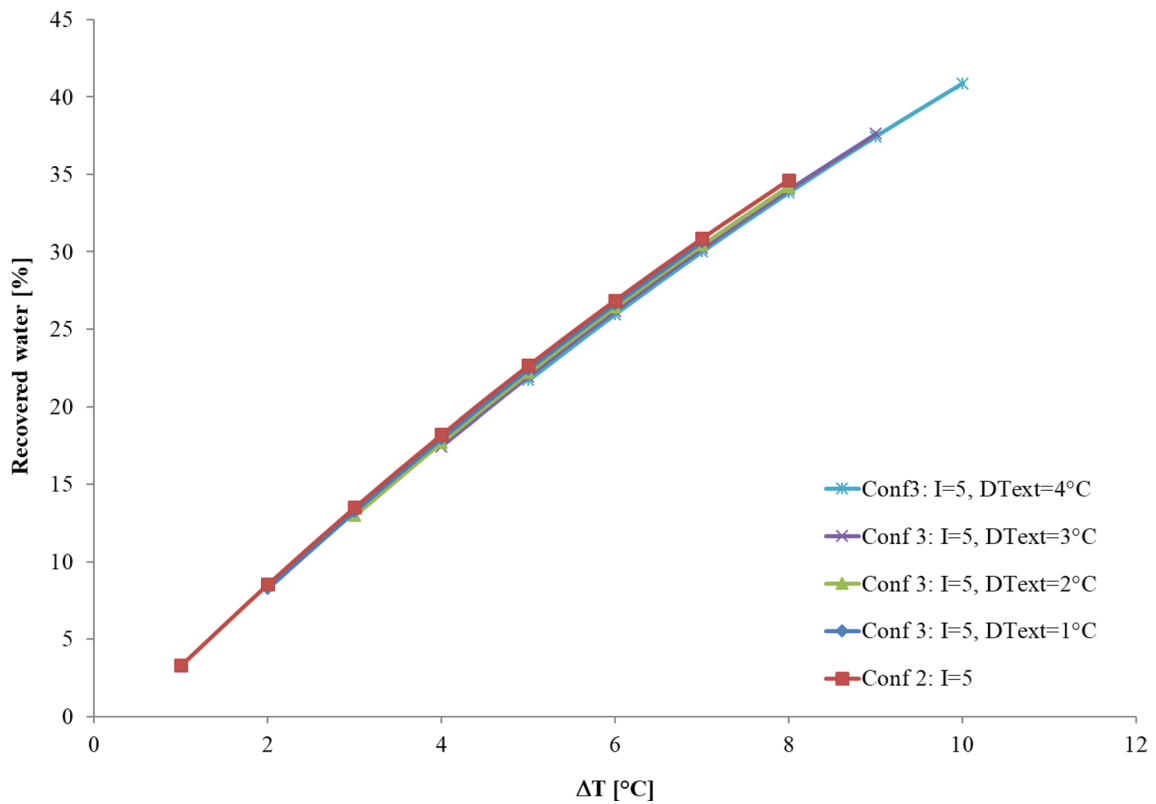


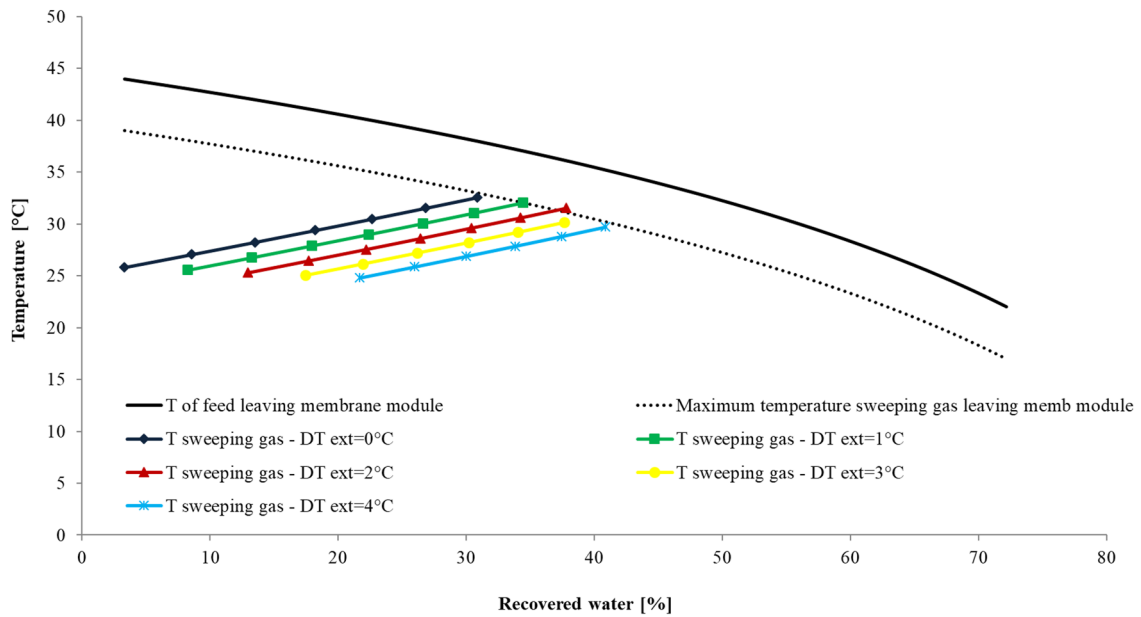
Fig. 7 Comparison of temperature and energy consumption for configuration 1 and 2. Feed temperature = 45 °C; RH feed = 100%



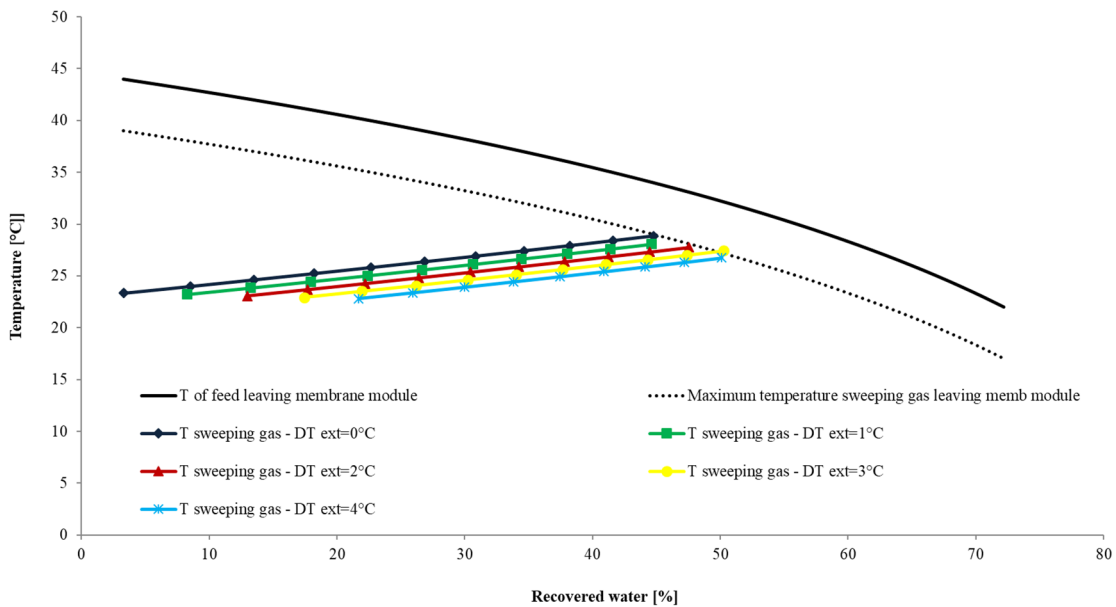
**Fig. 8** Ammonia concentration in recovered water as a function of feed cooling gradient ( $\Delta T$ ) and sweeping factor ( $I$ ) for configuration 2. (Feed temperature = 45  $^{\circ}\text{C}$ ; RH feed = 100%)



**Fig. 9** Recovered water versus  $\Delta T$  in configuration 3 and configuration 2 at  $I=5$  at increasing  $\Delta T_{\text{ext}}$  (the latter indicated as  $D_{\text{Text}}$  in the legend of the figure). Feed temperature = 45  $^{\circ}\text{C}$ ; RH feed = 100%



(a)



(b)

**Fig. 10** Temperature versus recovered water in configuration 3 at increasing  $\Delta T_{ext}$  (the latter indicated as DT<sub>ext</sub> in the legend of the figures): **a**  $I=5$ ; **b**  $I=10$ . Feed temperature = 45 °C; RH feed = 100%

refer to a feed at 45 °C and RH=100%, and supposing to utilize air at 20 °C as cold sweeping gas. In this case, the maximum water recovery is 22.7% if the air flow rate is

3 times that of feed ( $I = \text{sweeping factor} = 3$ ). Higher recovery cannot be obtained because the temperature difference

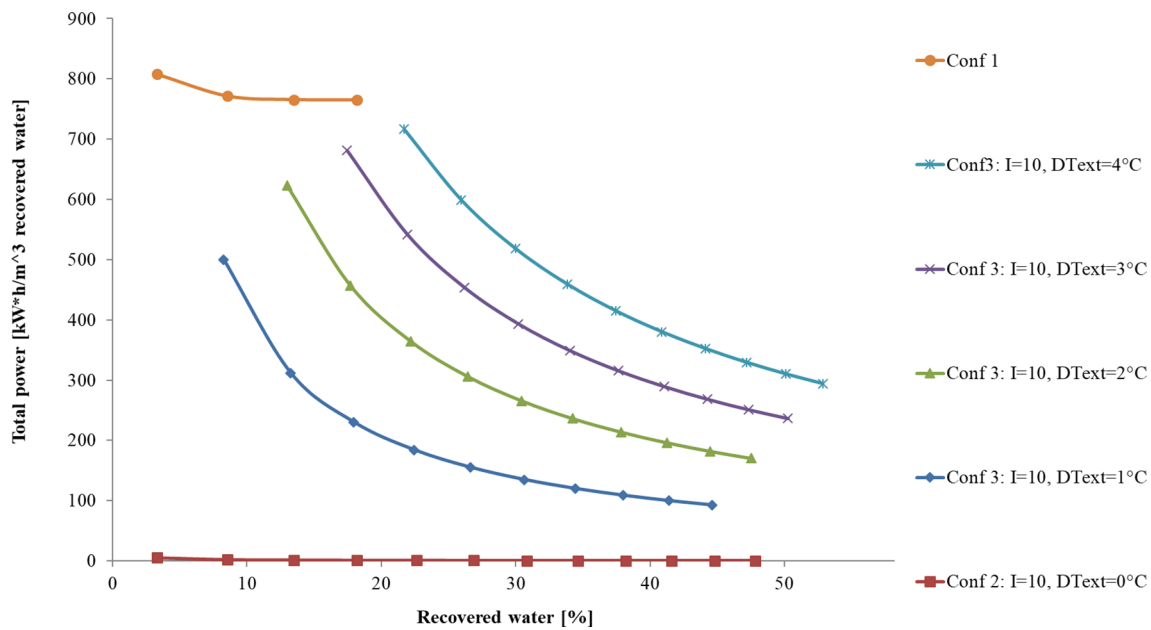


**Fig. 11** Energy consumption in configuration 3 versus configuration 1 and 2 at increasing  $\Delta T_{\text{ext}}$  (the latter indicated as  $D_{\text{Text}}$  in the legend of the figure). Feed:  $RH=100\%$ ,  $T=45\text{ }^{\circ}\text{C}$ ,  $I=10$

between the sweeping gas and the feed is not sufficient to achieve the condensation (Fig. 6b).

The results of the simulations indicated that in configuration 2, a higher water recovery (Fig. 7a) and lower energy consumption (Fig. 7b) can be achieved with respect to configuration 1.

Moreover, by increasing the sweeping factor  $I$ , the water recovery (Fig. 7a) and the maximum  $\text{NH}_3$  concentration (Fig. 8) increase. Finally, the comparison between Fig. 5 and Fig. 8 indicates that configuration 2 allows to recover a higher amount of  $\text{NH}_3$  than configuration 1 (about 38 ppm vs. about 27 ppm).

Configuration 3 (the one in which the feed is first partially cooled via an external medium and a sweeping gas is used for the final cooling of the stream), was analyzed considering an external cooling ( $\Delta T_{\text{ext}}$ ) from 0 to 4  $^{\circ}\text{C}$  and sweeping gas flow rate (for the internal cooling) in a range of sweeping factors from 1 to 10.

The patterns shown in Fig. 9 indicate that in configuration 3, a higher amount of water can be recovered compared to configuration 2. Moreover, at a constant  $I$ , water recovery increases with the increase in  $\Delta T_{\text{ext}}$  (Fig. 9), while for the same  $\Delta T_{\text{ext}}$ , water recovery increases with the increase in  $I$  (Fig. 10a, b).

The comparison of the three analyzed configurations in terms of energy consumption and concentration is shown in Figs. 11 and 12. Considering feed gas at 45  $^{\circ}\text{C}$  and  $RH=100\%$ , and air at 20  $^{\circ}\text{C}$  as cold sweeping gas (only for configurations 2 and 3), the highest energy consumption

is in configuration 1, while the lowest is in configuration 2 (Fig. 11).

For what concerns water recovery, the highest amount of liquid water can be obtained utilizing configuration 3 (with  $\Delta T_{\text{ext}}=4\text{ }^{\circ}\text{C}$  and  $I=10$ ) whose energy consumption ( $310\text{ kWh/m}^3_{\text{recovered water}}$ ) is in between configurations 1 and 2 (Fig. 11). Moreover, increasing  $I$  (Fig. 12), the  $\text{NH}_3$  concentration in the recovered liquid water will increase, too.

A comparison among the three different configurations in terms of water recovery, ammonia concentration and energy consumption is shown in Fig. 13. The comparison was made only at the conditions allowing to obtain the highest water recovery and ammonia concentration for each configuration. As it can be seen, the maximum amount of water recovery (50.1%) and ammonia concentration (40.5 ppm) can be obtained utilizing configuration 3 (with  $\Delta T_{\text{ext}}=4\text{ }^{\circ}\text{C}$ ) whose energy consumption ( $310\text{ kWh/m}^3_{\text{produced water}}$ ) is in between configuration 1 and configuration 2. However, configuration 2 is the one allowing to achieve the best compromise between energy consumption, water recovery and ammonia concentration. (Because with a 4.5% and 4.4% reduction in water recovery and ammonia concentration, respectively, the advantage due to the reduction in energy consumption is considerable).

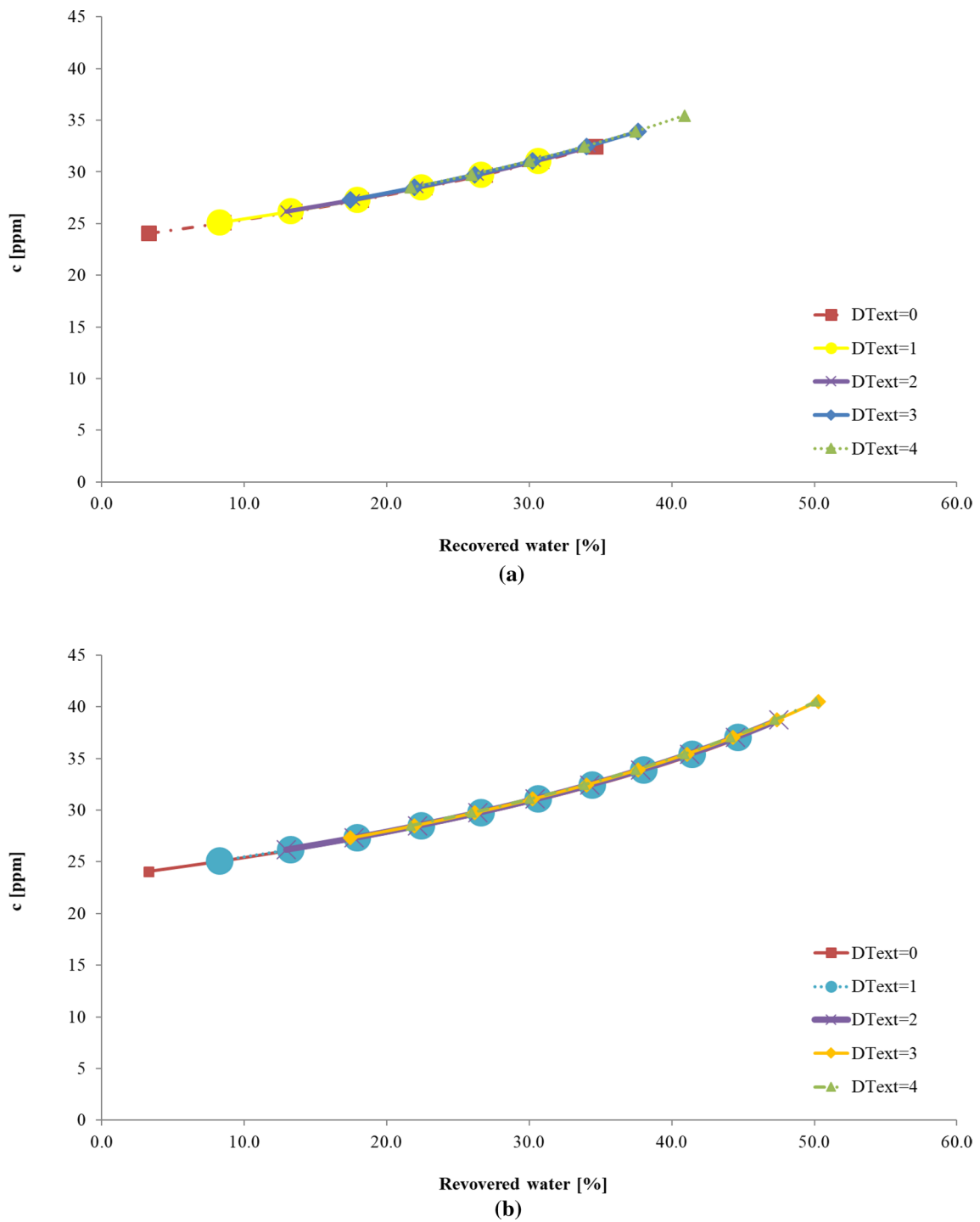
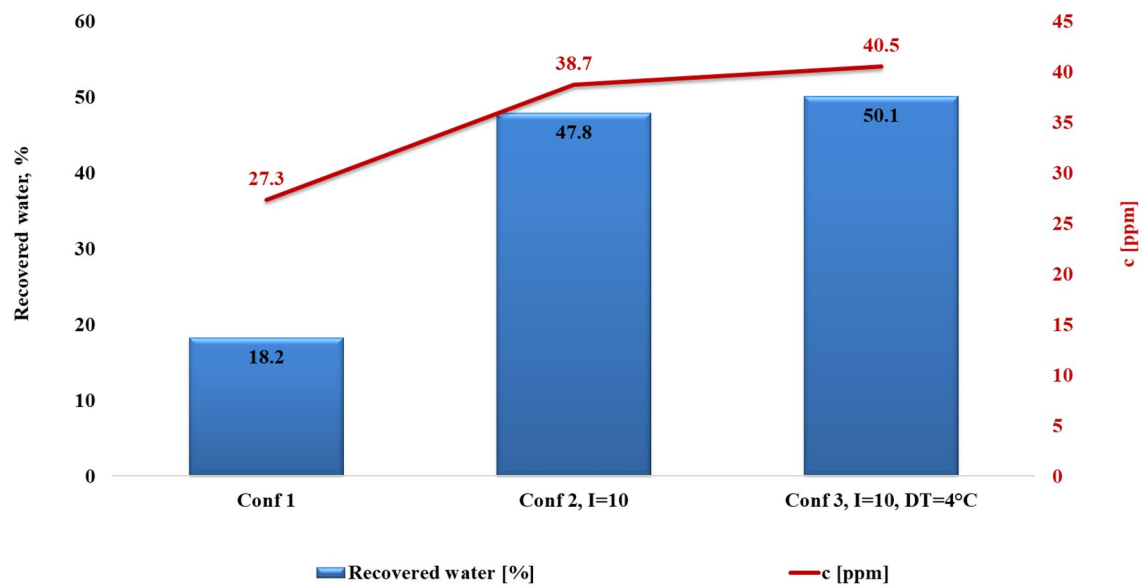


**Fig. 12** Variation of ammonia concentration in water recovered for configuration 3 at increasing  $\Delta T_{ext}$  (the latter indicated as DText in the legend of the figures) and at **a**  $I=5$  and **b**  $I=10$ . (Feed: RH = 100%,  $T=45$  °C)

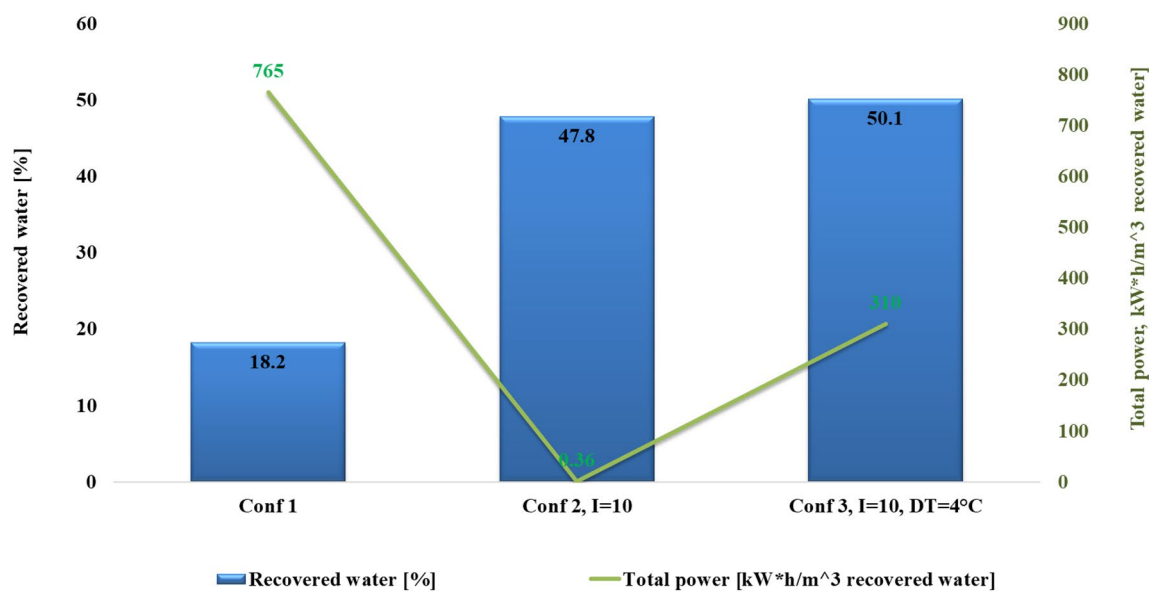
### Conclusions

In the present manuscript, the ability of the membrane condenser to recover ammonia from gas streams, with low energy consumption, has been analyzed. For achieving this

objective, three different possible membrane condenser configurations were considered: the fed gas was cooled via cooling water before entering the membrane module in configuration 1; cooling via a cold sweeping gas in the membrane module was utilized in configuration 2; a



(a)



(b)

**Fig. 13** Comparison among the three different configurations in terms of water recovery and **a** concentration, **b** energy consumption

combination of the first two cooling media was considered in configuration 3 (i.e. the fed waste gas is first partially cooled via an external medium and then a sweeping gas is used for the final cooling of the stream).

The process was analyzed both theoretically and experimentally. The carried out experiments allowed to validate the model, while the latter permitted to find the best configuration in terms of process energy consumption, quantity and concentration of the recovered water.

In the experiments as well as in the simulation,  $\Delta T$  indicates the temperature difference between the feed and the membrane module. It was observed that as  $\Delta T$  increases (keeping the temperature of the feed constant and reducing the temperature of the membrane module), both the saturation and the solubility of ammonia in the liquid water increase. Therefore, the results of the performed analyses

showed that water recovery and ammonia concentration increased with the increase in  $\Delta T$ .

As regards the different configurations studied, the achieved results indicated configuration 2, among the three different proposed schemes, the one that allows to minimize energy consumption while permitting a good recovery of water and chemicals.

**Funding** The authors extend their appreciation to the Deputyship for Research and Innovation, Ministry of Education in Saudi Arabia for funding this research work through the Project No. (421).

## Declarations

**Conflict of interest** The authors declare that they have no conflict of interest.

**Open Access** This article is licensed under a Creative Commons Attribution 4.0 International License, which permits use, sharing, adaptation, distribution and reproduction in any medium or format, as long as you give appropriate credit to the original author(s) and the source, provide a link to the Creative Commons licence, and indicate if changes were made. The images or other third party material in this article are included in the article's Creative Commons licence, unless indicated otherwise in a credit line to the material. If material is not included in the article's Creative Commons licence and your intended use is not permitted by statutory regulation or exceeds the permitted use, you will need to obtain permission directly from the copyright holder. To view a copy of this licence, visit <http://creativecommons.org/licenses/by/4.0/>.

## References

- Al-Odaidani S et al (2008) Potential of membrane distillation in seawater desalination: thermal efficiency, sensitivity study and cost estimation. *J Membr Sci* 323:85–98
- Bird RB, Stewart WE, Lighfoot EN (1960) *Transport Phenomena*. Wiley, New York
- Buijsman E, Maas HFM, Asman WAH (1987) Anthropogenic NH<sub>3</sub> emissions in Europe. *Atm Environ* 21:1009–1022
- Chang MB, Tseng TD (1996) Gas-phase removal of H<sub>2</sub>S and NH<sub>3</sub> with dielectric barrier discharges. *J Environ Eng* 122:41–46
- Clemens J, Cuhls C (2003) Greenhouse gas emissions from mechanical and biological waste treatment of municipal waste. *Environ Technol* 24:745–754
- Curcio E, Criscuoli A, Drioli E (2001) Membrane Crystallizers. *Ind Eng Chem Res* 40:2679–2684
- Enright R, Miljkovic N, Al-Obeidi A, Thompson CV, Wang EN (2012) Condensation on superhydrophobic surfaces: the role of local energy barriers and structure length scale. *Langmuir* 28(40):14424–14432
- Hasegawa T, Sato M (1998) Study of ammonia removal from coal-gasified fuel. *Combustion Flame* 114:246–258
- Haug RT (1993) *The Practical Handbook of Compost Engineering*. Lewis Publishers, Boca Raton, FL
- Hort C, Gracy S, Platel V, Moynault L (2009) Evaluation of sewage sludge and yard waste compost as a biofilter media for the removal of ammonia and volatile organic sulfur compounds (VOSCs). *Chem Eng J* 152:44–53
- Jun Y, Wenfeng X (2009) Ammonia biofiltration and community analysis of ammonia-oxidizing bacteria in biofilters. *Bioresour Technol* 100:3869–3876
- Kashchiev D (2000) *Nucleation: Basic Theory with Applications*, 1st edn. Butterworth-Heinemann, Oxford, U.K.
- Kim N-J, Hirai M, Shoda M (2000) Comparison of organic and inorganic packing materials in the removal of ammonia gas biofilters. *J Hazard Mater B* 72:77–90
- Kim JH, Rene ER, Park HS (2007) Performance of an immobilized cell biofilter for ammonia removal from contaminated air stream. *Chemosphere* 68:274–280
- La Pagans E, Font X, Sánchez A (2005) Biofiltration for ammonia removal from composting exhaust gases. *Chem Eng J* 113(2–3):105–110
- Lawson KW, Lloyd DR (1997) Membrane distillation. *Rev J Membr Sci* 124:1–25
- Macedonio F, Brunetti A, Barbieri G, Drioli E (2013) Membrane condenser as a new technology for water recovery from humidified “waste” gaseous streams. *Ind Eng Chem Res* 52(3):1160–1167
- Macedonio F, Cersosimo M, Brunetti A, Barbieri G, Drioli E (2014) Water recovery from humidified waste gas streams: quality control using membrane condenser technology. *Chem Eng Process* 86:196–203
- Macedonio F, Brunetti A, Barbieri G, Drioli E (2017) Membrane condenser configurations for water recovery from waste gases. *Sep Purif Technol* 181:60–68
- Macedonio F, Frappa M, Brunetti A, Barbieri G, Drioli E (2020) Recovery of water and contaminants from cooling tower plume. *Environ Eng Res* 25(2):222–229
- Malhautier L, Gracian C, Roux J-C, Fanlo J-L, Cloirec PL (2003) Biological treatment process of air loaded with an ammonia and hydrogen sulphide mixture. *Chemosphere* 50:145–153
- Mineral Commodity Summaries (2020), p 117 – Nitrogen” (PDF). USGS
- Moussavi G, Khavanin A, Sharifi A (2011) Ammonia removal from a waste air stream using a biotrickling filter packed with polyurethane foam through the SND process. *Bioresour Technol* 102(3):2517–2522
- Sakuma T, Jinsiriwanit S, Hattori T, Deshusses MA (2008) Removal of ammonia from contaminated air in a biotrickling filter–denitrifying bioreactor combination system. *Water Res* 42:4507–4513
- Wiwut T, Tawatchai C, Sahat C et al (2004) Effect of oxygen and water vapor on the removal of styrene and ammonia from nitrogen by non-pulse corona discharge at elevated temperature. *Chem Eng J* 97:213–223
- Xia L, Huang L, Shu X, Zhang R, Dong W, Hou H (2008) Removal of ammonia from gas streams with dielectric barrier discharge plasmas. *J Hazard Mater* 152(1):113–119
- Yasuda T, Kuroda K, Fukumoto Y, Hanajima D, Suzuki K (2009) Evaluation of full-scale biofilter with rockwool mixture treating ammonia gas from livestock manure composting. *Bioresour Technol* 100:1568–1572

**Publisher's Note** Springer Nature remains neutral with regard to jurisdictional claims in published maps and institutional affiliations.